

Diethylene Glycol Diethyl Ether as Electrolyte Solvent for Reversible Electrochemical Magnesium Plating

Benjamin W. Schick, Matthias Uhl, Mohammad Al-Shakran, Joachim Bansmann, Sibylle Riedel, Zhirong Zhao-Karger, and Timo Jacob*

Due to their high theoretical energy density and the abundance of magnesium, rechargeable Mg batteries are promising candidate systems for future energy storage. However, finding suitable electrolytes that are compatible with the metallic Mg electrode and enable highly reversible Mg plating is still challenging. Typical electrolytes for rechargeable magnesium batteries are based on ether solvents such as tetrahydrofuran (THF), dimethoxyethane (DME), or higher glymes. Drawbacks are the high volatilities and low flashpoints of THF and DME and their harmfulness, problematic factors for industrial applicability. One potential alternative is diethylene glycol diethyl ether

(DEGDDE) which is also an ether, but has significantly higher boiling and flashpoints than THF and DME, and is from today's perspective less harmful than any of the previously mentioned solvents. To test the suitability and stability of this class of electrolytes, different Mg salts in combination with DEGDDE for their electrochemical Mg plating and stripping properties are studied. Although Mg deposition needs higher overpotentials than for their DME-based counterparts, the investigated electrolytes enable reversible Mg plating with relatively high Coulombic efficiencies, making DEGDDE a promising alternative electrolyte solvent for rechargeable Mg batteries.

1. Introduction

Electrochemical energy storage, especially Li-ion batteries (LIB), are an integral part of today's world and are playing an increasingly important role. Examples include portable electronic devices, battery electric vehicles, and stationary energy storage applications.^[1,2] Besides LIBs, new technologies are emerging, which could offer improved properties such as higher energy densities, abundance of raw materials, and higher safety.^[3–5] Among them, rechargeable magnesium batteries (RMBs) are

gaining more attention as Mg offers a high theoretical energy density and abundance.^[6,7] However, RMBs are still in their infancy and a number of challenges need to be overcome for realizing their practical application.^[3,7] In addition to the search for high-potential cathode materials, the development of suitable electrolytes is one of the key tasks.^[8] The electrolytes have to enable highly reversible and smooth electrochemical magnesium deposition without forming passivation layers.^[9,10] This is only possible if the electrolyte components are stable toward metallic magnesium, meaning that most of the typical electrolytes which are applied in LIBs are impractical for RMBs.^[6,10,11] Among them are carbonate- and ester-based electrolytes which form passivation layers that block the deposition and dissolution of Mg.^[3,12] Furthermore, typical salts, such as $\text{Mg}(\text{PF}_6)_2$ and $\text{Mg}(\text{ClO}_4)_2$, react with metallic Mg and are not suitable as electrolyte components.^[9]

One of the very few classes of solvents which, in combination with suitable salts, show good compatibility with metallic Mg are ethers. The ethers being used most as solvent for Mg electrolytes to date are tetrahydrofuran (THF) and dimethoxyethane (DME, monoglyme).^[13–15] In combination with certain Mg salts, such as magnesium tetrakis (hexafluoroisopropoxy) borate ($\text{Mg}[\text{B}(\text{hfp})_4]_2$), all phenyl complex (APC), or magnesium bis (hexamethyldisilazide) ($\text{Mg}(\text{HMDS})_2$)/ MgCl_2 , they show relatively high ionic conductivities and good performance in Mg plating and stripping.^[16–19] The drawbacks of these solvents are low boiling points and high flammability. These cause problems in terms of safety and commercialization.^[20–24] Furthermore, they are chemicals of high concern and are hence also problematic for regulatory reasons.^[25] Alternative solvents which have been successfully studied for Mg plating include higher glymes such as diglyme, triglyme, or tetraglyme. In combination with suitable Mg salts, they enable Mg plating and stripping and show high


B. W. Schick, M. Uhl, M. Al-Shakran, T. Jacob
Institute of Electrochemistry
Ulm University
Albert-Einstein-Allee 47, 89081 Ulm, Germany
E-mail: timo.jacob@uni-ulm.de


J. Bansmann
Institute of Surface Chemistry and Catalysis
Ulm University
Albert-Einstein-Allee 47, 89081 Ulm, Germany

S. Riedel, Z. Zhao-Karger, T. Jacob
Helmholtz-Institute Ulm (HIU) Electrochemical Energy Storage
Helmholtzstr. 11, 89081 Ulm, Germany

Z. Zhao-Karger
Institute of Nanotechnology
Karlsruhe Institute of Technology (KIT)
P.O. Box 3640, 76021 Karlsruhe, Germany

T. Jacob
Karlsruhe Institute of Technology (KIT)
P.O. Box 3640, 76021 Karlsruhe, Germany

 Supporting information for this article is available on the WWW under <https://doi.org/10.1002/celc.202500046>

 © 2025 The Author(s). ChemElectroChem published by Wiley-VCH GmbH. This is an open access article under the terms of the Creative Commons Attribution License, which permits use, distribution and reproduction in any medium, provided the original work is properly cited.

conductivity.^[26–29] However, despite their higher boiling points and good electrochemical performance, these ethers are also chemicals of high concern.^[30] Besides ethers, Mg plating from ionic liquid-based electrolytes has also been demonstrated. Ionic liquids have beneficial safety properties, such as low flammability and nonvolatility.^[23] At the same time their high viscosity is a drawback, which is why they are often used in combination with ether cosolvents.^[31–33] So far, the ionic-liquid-based Mg electrolytes have not prevailed due to the usually limited performance in Mg plating and stripping and higher costs.^[23,33]

In the perspective article of Blázquez et al.^[7] several improvements and changes in RMB components, such as Mg salts and cathodes, are predicted for improving the performance of RMBs. But in their forecast, exclusively THF and DME are discussed due to the lack of suitable alternatives. However, improvements in this area are also essential for a successful commercialization of RMBs.^[10,25]

In this regard, diethylene glycol diethyl ether (DEGDEE) is a promising candidate as possible solvent for Mg electrolytes. DEGDEE is also an ether solvent, but in contrast to THF or DME, less toxic, has a significantly higher boiling point, lower vapor pressure, and higher flashpoint as shown in **Figure 1**.^[20,24,34,35] The comparison of the structural formulae of DEGDEE and DME is also illustrated in Figure 1. Although the vapor pressure of the structurally related diglyme is still three times higher than that of DEGDEE, one has to mention that higher glymes show comparable or even lower vapor pressure.^[13,30] However, from today's perspective, DEGDEE is less toxic than the other mentioned glymes.^[25,30]

DEGDEE-based electrolytes have already been investigated for LIBs and show promising properties.^[20,34,36] There, the DEGDEE-based electrolytes showed a broad electrochemical stability window, comparable to other glymes,^[36] meaning that Mg plating and stripping should occur within the electrochemical stability window of the solvent. Therefore, the question arises whether DEGDEE could also be a suitable electrolyte solvent for reversible Mg plating with regard to the application in RMBs.

For our study, we have chosen three typical Mg salts which have shown reversible Mg plating and stripping with DME as solvent. The investigated Mg salts for the combination with DEGDEE are Mg(HMDS)₂, magnesium bis (trifluoromethanesulfonyl) imide (Mg(TFSI)₂), and Mg[B(hfp)₄]₂. In combination with DME, they show relatively high Coulombic efficiencies well over 90% for Mg plating and stripping, especially when they are combined with MgCl₂.^[16,18,19,37,38] The choice of the three different salts makes it possible to test DEGDEE for its general applicability

as an electrolyte solvent for Mg plating and stripping. Furthermore, we compared the influence of the different Mg salts on the electrochemical performance and the morphology of the deposits.

Borohydrides as an additive help to scavenge electrolyte impurities, such as H₂O, which leads to smoother Mg plating and higher Coulombic efficiencies.^[39,40] Therefore, we have added a small amount of tetrabutylammonium borohydride (TBABH₄) to all of our electrolytes in this study.

Cyclic voltammetry, galvanostatic plating and stripping cycles, and X-ray photoelectron spectroscopy (XPS) and scanning electron microscopy (SEM) with energy-dispersive spectroscopy (EDS) of the deposits show the ability to deposit metallic Mg electrochemically from all investigated DEGDEE-based electrolytes. Mg plating and stripping occurs with relatively high Coulombic efficiencies when using Mg(HMDS)₂/MgCl₂ or Mg[B(hfp)₄]₂ as electrolyte salts, even comparable to the DME-based counterparts. However, due to lower electrolyte conductivities, the overpotentials are relatively high compared to the DME-based electrolytes, which emphasizes the need of further optimization to achieve practical application of less critical DEGDEE in RMBs.

2. Results and Discussion

The first Mg salt of choice was Mg(HMDS)₂ which shows relatively good performance with respect to Mg plating and stripping in DME.^[38,41] It is known that the addition of MgCl₂ significantly improves the performance in Mg electrolytes; therefore, we used a mixture of these salts for our studies.^[19,41] The electrolyte was prepared by dissolving 0.14 M Mg(HMDS)₂, 0.14 M MgCl₂, and 15 mM TBABH₄ in DEGDEE. For comparison, a DME-based electrolyte with the same salt combination was used as benchmark. The Mg(HMDS)₂/MgCl₂ combination was less soluble in DME than in DEGDEE; therefore, this electrolyte had concentrations of 0.1 M Mg(HMDS)₂, 0.05 M MgCl₂, and 15 mM TBABH₄.

Cyclic voltammetry was performed in a three-electrode setup to test the ability of the DEGDEE-based electrolyte to reversibly deposit Mg. **Figure 2** shows typical cyclic voltammograms of the electrolyte, using a platinum working electrode at a scan rate of 25 mV s⁻¹. During the negative scan, Mg deposition starts with an overpotential of about 200 mV vs. Mg. The presumption that the observed currents are attributed to Mg deposition was confirmed with EDS (Figure S1, Supporting Information). For the initial nucleation, a higher overpotential is needed, which is typical for Mg plating.^[8,19,42] In the positive scan in Figure 2, Mg dissolution is starting at slightly negative potentials vs. Mg. The Mg/Mg²⁺ redox potential is shifted negatively compared to the 0 V one would expect for a Mg metal reference electrode. The reason for this is most probably passivation of the Mg reference electrode which leads to a positive potential shift compared to freshly deposited Mg as found by Yoo and co-authors.^[43] Similar to the Mg deposition, the overpotential for the dissolution is relatively large, and the stripping is not completed until >1 V vs. Mg. Compared to the best performing electrolytes, such as Mg[B(hfp)₄]₂ in DME, the current density in the investigated potential range is significantly lower, assumed that the setups are comparable.^[16] The different

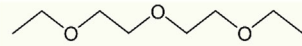
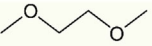


	
DEGDEE	DME
0.79 hPa	77.8 hPa
189 °C	84 °C
70 °C	-2 °C
	
Vapour pressure (20 °C)	
Boiling point	
Flash point	
Hazards	

Figure 1. Structural formulae and selected properties of the solvents DEGDEE and DME.^[20,24,35]

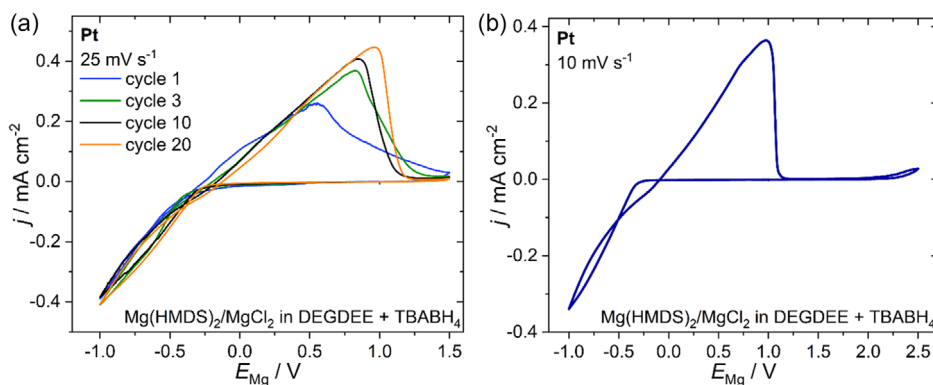


Figure 2. a) Cyclic voltammogram of selected cycles of the initial 20 cycles with the 0.14 M Mg(HMDS)₂/0.14 M MgCl₂/15 mM TBABH₄ electrolyte in DEGDEE with a Pt working electrode and a scan rate of 25 mV s⁻¹. b) Corresponding typical cyclic voltammogram of the conditioned electrolyte with a scan rate of 10 mV s⁻¹.

current densities are most probably a result of different electrolyte conductivities. Mg[B(hfp)₄]₂ in DME has an electrolyte conductivity of several mS cm⁻¹,^[27,37,39,44] while the DEGDEE-based Mg(HMDS)₂/MgCl₂ electrolyte has a conductivity of about 34 ± 4 μS cm⁻¹ at room temperature. Despite the lower solubility of these salts in DME, the corresponding DME electrolyte also showed higher ionic conductivity (0.28 ± 0.03 mS cm⁻¹), which is in agreement with similar electrolytes reported in literature.^[41] The clear difference in conductivity is also reflected when comparing the potentiostatic impedance spectra at open circuit potential (Figure S2, Supporting Information). One reason for the difference in conductivity is the three times higher viscosity of pure DEGDEE compared to DME.^[20] Generally, the viscosity increases with an increasing glyme length.^[27] But the high conductivity of Mg[B(hfp)₄]₂ in DME means that the Mg salt and its solvation, mobility, and contact ion pair formation in the respective solvent also play a crucial role for the overall electrolyte conductivity.^[45]

Figure 2a shows that the reversibility of the plating and stripping processes is lower in the first cycle at ≈86%. It increases during the initial cycles and the Coulombic efficiency stabilizes at high values of about 97% after 20 cycles (Figure S3, Supporting Information). From literature this is known as the conditioning process during which most probably impurities react with Mg to form a passivation layer which afterward degrades if the electrolyte itself is electrochemically stable.^[46] It can also be seen that the dissolution peak is getting sharper during this process, which means that the current density drops faster after the maximum peak current. TBABH₄ as additive should scavenge most of the residual H₂O in the electrolyte. However, since both Mg(HMDS)₂ and DEGDEE are commercially not available in highest purities, the presence of other electrolyte impurities that react with Mg cannot be excluded. The conditioning process is less pronounced in the DME-based electrolyte (Figure S4, Supporting Information), which could be explained by a higher purity of DME compared to DEGDEE (99% for DEGDEE vs. 99.5% for DME). At positive potentials, DEGDEE itself is supposed to be stable against oxidation,^[36] where the limited anodic stability is most likely related to the presence of borohydrides.^[47] To achieve a broader electrochemical stability window, the borohydride

concentration could be tuned to achieve an optimum balance between the impurity scavenging effect and the anodic stability.^[29,48]

To further examine the Coulombic efficiency of the plating and stripping process, macrocycling experiments in a two-electrode setup were conducted as suggested by Attias et al.^[49,50] In these experiments, a reservoir of Mg is deposited electrochemically (−200 μA cm⁻² for 1 h). Subsequently, 5% of this amount is repeatedly stripped and plated for 100 cycles (±200 μA cm⁻² for 3 min). In the final step, Mg is dissolved electrochemically until the cut-off voltage of 2 V is reached. The Coulombic efficiency is determined by the fraction of overall stripping charges and plating charges.^[49] Figure 3 shows the potential profiles for the galvanostatic macrocycling experiments with 5% depth of discharge. As the initial conditioning step, five plating and stripping cycles were carried out with a current density of ±200 μA cm⁻² for 3 min each and a cut-off voltage of 2 V (Figure S5, Supporting Information). As a benchmark, the same procedure was performed with the DME-based electrolyte (Figure 2b) in addition to the DEGDEE electrolyte. As expected from the lower conductivity, the overpotentials for Mg plating and stripping are significantly higher for the DEGDEE-based electrolyte compared to the DME-based counterpart. The macrocycling experiment was performed at a relatively low current density of 200 μA cm⁻², as higher currents would have led to even higher overpotentials in the DEGDEE-based electrolyte. For the DME electrolyte (Figure 3b), the overpotentials are relatively low, which is consistent with reports from literature.^[41] But despite the differences in overpotential, the Coulombic efficiency in the macrocycling experiment is between 97 and 98% in both cases. This is relatively high and no significant differences were observed between the DME- and the DEGDEE-based electrolytes. The similar Coulombic efficiencies show that both ethers are equally stable and there are no significant amount of side reactions taking place in both electrolytes. Therefore, DEGDEE can indeed compete with DME in this regard.

The potential decomposition of ether solvents has so far predominantly been the subject of theoretical studies.^[51–53] Possible degradation pathways of ethers, such as DME, include the decomposition under evolution of ethylene gas and the

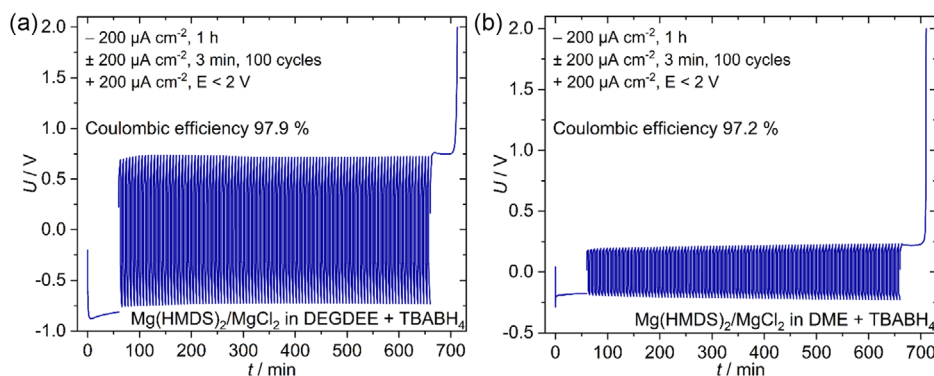


Figure 3. a) Voltage profile of the macrocycling experiment in a two-electrode setup with Pt and Mg electrode for the conditioned 0.14 M Mg(HMDS)₂/0.14 M MgCl₂/15 mM TBABH₄ electrolyte in DEGDEE. b) Voltage profile of the macrocycling experiment in a two-electrode setup with Pt and Mg electrode for the conditioned 0.1 M Mg(HMDS)₂/0.05 M MgCl₂/15 mM TBABH₄ electrolyte in DME.

formation of Mg(OCH₃)₂(DME)₂ species that block the Mg surface^[52,53] and the reaction between ethers and partially reduced Mg cations via cleavage of the C–O bond.^[51] However, no indications of solvent decomposition were found in our experiments, including nuclear magnetic resonance (NMR) spectroscopy (Figure S6, Supporting Information).

The comparison between the investigated DEGDEE-based electrolyte and other electrolytes from literature which are based on DME and higher glymes is difficult because of the huge variety in electrolyte composition and experimental conditions. Generally speaking, glymes enable Mg plating and stripping and appear to be stable toward metallic Mg. The Coulombic efficiency and conductivity is rather driven by the Mg salts with which the ethers are combined.^[26,28,29,47,54–56] While the Coulombic efficiency was relatively low with higher glymes in combination with Mg(TFSI)₂, high Coulombic efficiencies and conductivities were reached with stable and weakly coordinating salts, such as Mg[B(hfip)₄]₂ and similar alkoxyaluminate salts.^[27–29,54,57]

To investigate the ability of DEGDEE to dissolve further commonly used Mg salts, Mg[B(hfip)₄]₂ and Mg(TFSI)₂ were also explored by preparing the corresponding electrolytes. Mg[B(hfip)₄]₂ has gained increasing attention within the last years

due to its good electrochemical stability and performance for Mg plating and stripping.^[14,16,44,48] In our case, each Mg[B(hfip)₄]₂ is complexed with three DME molecules due to the synthesis process. The salt is well soluble in DEGDEE and we prepared a mixture of 0.14 M Mg[B(hfip)₄]₂·3DME and 20 mM TBABH₄ in DEGDEE. This means that the electrolyte is chloride free in contrast to the previously described Mg(HMDS)₂-containing electrolyte, which is an advantage due to the corrosiveness of chloride toward stainless steel and aluminum cell components.^[58] For the sake of comparability and to elucidate the impact of the DME, we also prepared a pure DME electrolyte with the same salt concentrations. **Figure 4a** shows two typical cyclic voltammograms of the DEGDEE and the DME electrolytes. As for the Mg(HMDS)₂/MgCl₂ electrolyte, the plating charge and Coulombic efficiency increases within the initial cycles (Figure S7, Supporting Information). For the same negative potential limit as with the Mg(HMDS)₂-based electrolyte, the plating and stripping currents are significantly higher with the Mg[B(hfip)₄]₂-based electrolyte. For Mg[B(hfip)₄]₂ with DEGDEE, there is a peak in the Mg deposition region of the negative scan at about –0.5 V vs. Mg as well as a shoulder in the Mg dissolution in the positive scan at about 0.3 V vs. Mg. The comparison with the corresponding DME-based electrolyte reveals that these peaks are most probably attributed

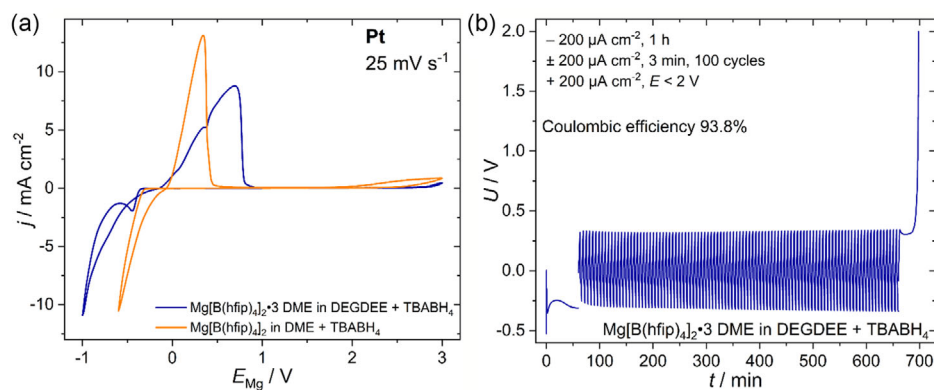


Figure 4. a) Typical cyclic voltammogram of the conditioned 0.14 M Mg[B(hfip)₄]₂·3DME/20 mM TBABH₄ electrolyte in DEGDEE and in DME with a Pt working electrode and a scan rate of 25 mV s^{–1}. b) Voltage profile of the macrocycling experiment of the conditioned 0.14 M Mg[B(hfip)₄]₂·3DME/20 mM TBABH₄ electrolyte in DEGDEE.

to the deposition from the limited number of DME complexes in the electrolyte which apparently require a lower overpotential compared to the DEGDEE complexes. The conductivity of the $\text{Mg}[\text{B}(\text{hfp})_4]_2/\text{DME}$ electrolyte is $7 \pm 0.7 \text{ mS cm}^{-1}$ and that of the $\text{Mg}[\text{B}(\text{hfp})_4]_2/\text{DEGDEE}$ electrolyte is $2 \pm 0.2 \text{ mS cm}^{-1}$. Similar to the $\text{Mg}(\text{HMDS})_2/\text{MgCl}_2$ electrolytes, the DME variant therefore has a higher conductivity than the DEGDEE one, which is also reflected in the cyclic voltammogram and in comparison with PEIS spectra (Figure S8, Supporting Information). This means that the solvation shell of the ethers around the Mg salt in the electrolyte obviously plays an important role for the electrolyte conductivity and the plating and stripping overpotentials. Due to the different denticities and chelations with different glyme lengths (DME bidentate vs. DEGDEE tridentate), different coordination structures were observed.^[45] However, studies on diglyme-based electrolytes with $\text{Mg}[\text{B}(\text{hfp})_4]_2$ and similar Mg salts revealed that these electrolytes show even lower overpotentials than the DME-based ones and an overall good performance with Coulombic efficiencies of nearly 100%.^[27,54,59] This means that the terminal ethoxy group of DEGDEE might be unfavorable in this aspect compared to the methoxy groups of DME and diglyme. The macrocycling experiment with the same conditions as for the $\text{Mg}(\text{HMDS})_2/\text{MgCl}_2$ electrolyte also shows low overpotentials for Mg plating and stripping. The Coulombic efficiency of 93.8% is in the range of the already reported Coulombic efficiency for the $\text{Mg}[\text{B}(\text{hfp})_4]_2$ electrolyte in DME from macrocycling experiments.^[49] At the same time, it is a little lower compared to a report where the Coulombic efficiency of a $\text{Mg}[\text{B}(\text{hfp})_4]_2/\text{MgBH}_4$ electrolyte in DME was determined by cyclic voltammetry.^[48] With the $\text{Mg}[\text{B}(\text{hfp})_4]_2 \cdot 3\text{DME}/\text{DEGDEE}$ electrolyte, it was also possible to perform the macrocycling measurement at higher current densities due to the higher conductivity compared to the $\text{Mg}(\text{HMDS})_2/\text{MgCl}_2$ electrolyte with DEGDEE. The macrocycling experiment with the same conditions, but with a current density of 1 mA cm^{-2} , led to a Coulombic efficiency of even 96.5% (Figure S9, Supporting Information). A higher concentration of 0.3 M $\text{Mg}[\text{B}(\text{hfp})_4]_2 \cdot 3\text{DME}$ in DEGDEE was also soluble and showed a Coulombic efficiency of about 95% in the macrocycling experiment with a current density of $200 \mu\text{A cm}^{-2}$ (Figure S9, Supporting Information).

During the conditioning cycles (Figure S10, Supporting Information), the Coulombic efficiency is low in the first cycle (60%) and increases even after five cycles. The reason for the more pronounced conditioning behavior could be the lack of chloride.^[46] The addition of MgCl_2 would most probably minimize the conditioning process and further improve the performance of this electrolyte.^[37,46]

The overall performance of the DEGDEE electrolyte with $\text{Mg}[\text{B}(\text{hfp})_4]_2$ is convincing as it combines good solubility with good electrochemical performance in terms of conductivity, plating and stripping overpotential, and Coulombic efficiency. Nevertheless, it does not reach the performance of the DME counterpart with respect to conductivity.

The third salt of choice is $\text{Mg}(\text{TFSI})_2$ which is frequently used, especially in combination with MgCl_2 .^[19] $\text{Mg}(\text{TFSI})_2$ is not well soluble in DEGDEE, so the concentration was only 0.05 M each for $\text{Mg}(\text{TFSI})_2$ and MgCl_2 . Again, we added 15 mM TBABH₄ to the $\text{Mg}(\text{TFSI})_2$ -based electrolyte to scavenge water impurities. Figure 5 shows a typical cyclic voltammogram after the initial conditioning cycles (Figure S11, Supporting Information). Mg plating and stripping also take place in this electrolyte, but the Coulombic efficiency is significantly lower (about 86% in the cyclic voltammogram in Figure 5a) than for the $\text{Mg}(\text{HMDS})_2/\text{MgCl}_2$ - and the $\text{Mg}[\text{B}(\text{hfp})_4]_2$ -based electrolytes. Although the solubility of the $\text{Mg}(\text{TFSI})_2/\text{MgCl}_2$ mixture is very low compared to the other investigated salts, the conductivity is still clearly higher than for the $\text{Mg}(\text{HMDS})_2/\text{MgCl}_2$ electrolyte, which is reflected in the overpotentials and current densities for Mg deposition and in the impedance spectra (Figure S5 and S9, Supporting Information). The clearly lower Coulombic efficiency is also evident in the macrocycling experiment (Figure 5b). The plating and stripping during the 100 cycles already exceed the given potential limits (-2 V for $-200 \mu\text{A cm}^{-2}$ and $+2 \text{ V}$ for $+200 \mu\text{A cm}^{-2}$) which results in a Coulombic efficiency of 57% when the charges up to the 30th dissolution step are considered. The current limit is first reached for the dissolution of Mg from the Pt electrode after 20 cycles, which means that the active Mg is depleted. About ten cycles later, the current limit of -2 V is also exceeded for the Mg plating steps. One reason for this is most probably a thick passivation layer of irreversibly

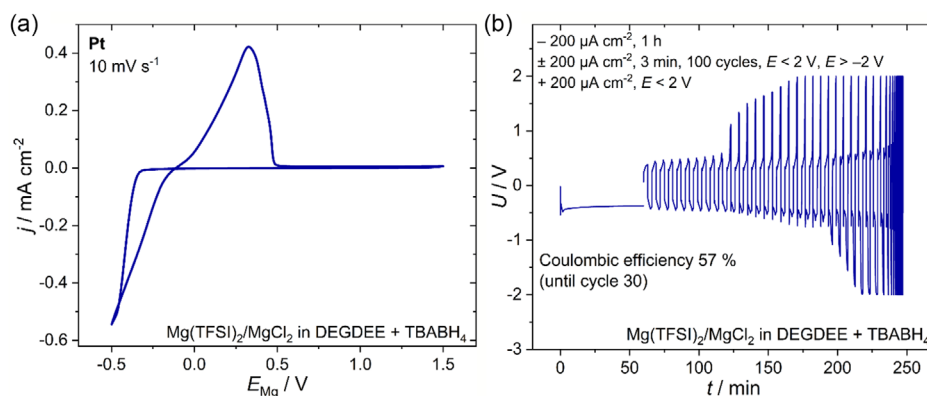


Figure 5. a) Typical cyclic voltammogram of the conditioned 0.05 M $\text{Mg}(\text{TFSI})_2/0.05 \text{ M MgCl}_2/15 \text{ mM TBABH}_4$ electrolyte in DEGDEE with a scan rate of 10 mV s^{-1} . b) Voltage profile of the macrocycling experiment of the conditioned 0.05 M $\text{Mg}(\text{TFSI})_2/0.05 \text{ M MgCl}_2/15 \text{ mM TBABH}_4$ electrolyte in DEGDEE.

deposited Mg due to side reactions between electroplated Mg and the electrolyte, which hinders further Mg plating.^[46] Furthermore, the passivation of the Mg counter electrode leads to highly positive potentials of the counter electrode during the deposition process on the working electrode. The Coulombic efficiency with this electrolyte is also considerably lower than for the $\text{Mg}(\text{TFSI})_2/\text{MgCl}_2$ electrolytes with DME as solvent.^[19,49] One explanation could be the formation of contact ion pairs and the resulting higher reactivity of undercoordinated $[\text{MgTFSI}]^+$ complexes in the DEGDEE electrolyte.^[60,61] In electrolytes with $\text{Mg}(\text{TFSI})_2$ which is dissolved in higher glymes the Coulombic efficiency did not exceed 80% either.^[28,29,57,62]

To sum up the comparison of the electrochemical results of the three different DEGDEE-based electrolytes, all investigated electrolytes show mostly reversible Mg plating and stripping. The $\text{Mg}(\text{HMDS})_2/\text{MgCl}_2$ electrolyte is characterized by a high Coulombic efficiency although the electrolyte conductivity is relatively low and therefore the overpotentials are high. The $\text{Mg}(\text{TFSI})_2/\text{MgCl}_2$ salts have a low solubility in DEGDEE but a higher conductivity than the $\text{Mg}(\text{HMDS})_2/\text{MgCl}_2$ electrolyte. However, the Coulombic efficiency is significantly lower and therefore this electrolyte would be unsuitable as electrolyte for RMBs. The $\text{Mg}[\text{B}(\text{hfp})_4]_2$ electrolyte shows a relatively high conductivity and Coulombic efficiency and is a promising

candidate whose performance could be even enhanced by the addition of MgCl_2 .

In addition to the electrochemical measurements, the morphology of the electrodeposited Mg was also investigated and compared. The procedure was the same for all three electrolytes. After an initial impedance spectrum, again five plating and stripping cycles were carried out under the same conditions as for the macrocycling experiment (Figure S12, Supporting Information). Subsequently, Mg plating was done with a current density of $-200 \mu\text{A cm}^{-2}$ for 1 h. Figure 6 shows the SEM images of the corresponding Mg deposits. In all three electrolytes, the plated Mg was evenly distributed on the whole electrochemical active surface area and the deposits had the same morphology on the whole surface for the respective electrolytes (Figure S13, Supporting Information). The bright fibers in the images are leftovers of the glass fiber separator. In general, the deposition morphology strongly depends on the electrolyte species, the Mg salt concentration, and the deposition current.^[39,49] The underlying deposition mechanisms are not yet fully understood, but it is clear that even low levels of impurities have a major influence on the morphology of the deposits.^[39,63] Side reactions during Mg plating and the resulting passivation layers might lead to less dense deposits and filamentary growth, whereas efficient electroplating with few side reactions leads to more densely packed Mg

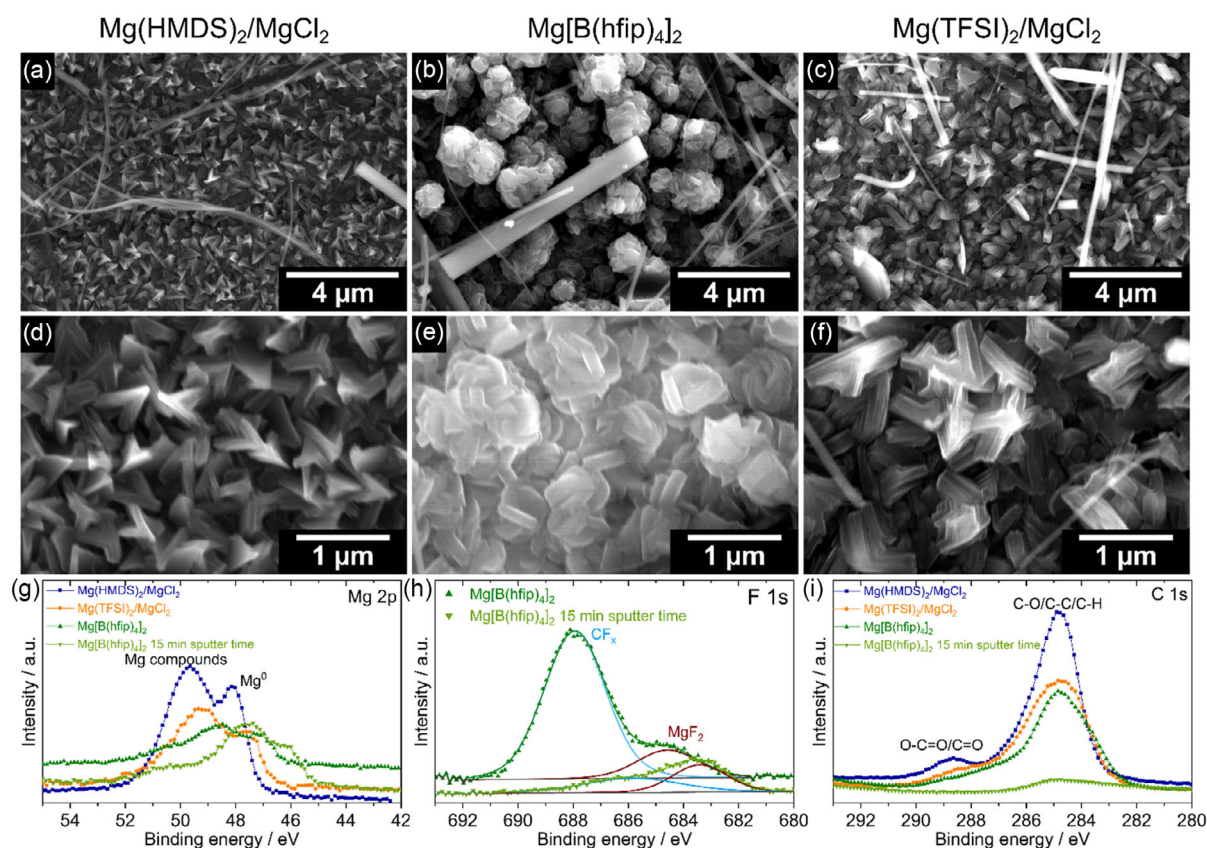


Figure 6. SEM images of the electrodeposited Mg after five galvanostatic conditioning cycles and a deposition current density of $-200 \mu\text{A cm}^{-2}$ for 1 h: a,d) electrodeposition from the $\text{Mg}(\text{HMDS})_2/\text{MgCl}_2/\text{TBABH}_4$ electrolyte in DEGDEE; b,e) electrodeposition from the $\text{Mg}[\text{B}(\text{hfp})_4]_2/\text{TBABH}_4$ electrolyte in DEGDEE; and c,f) electrodeposition from the $\text{Mg}(\text{TFSI})_2/\text{MgCl}_2/\text{TBABH}_4$ electrolyte in DEGDEE. g,h,i) Detailed XPS spectra of the Mg deposits from the different electrolytes for Mg 2p (g), F 1s (h) and C 1s (i). For the deposit from the $\text{Mg}[\text{B}(\text{hfp})_4]_2$ -based electrolyte, the spectra of the fresh surface (dark green) and after 15 min of sputtering (light green) are shown.

deposits.^[46,49] It was further observed that the shape of the deposits is influenced by the presence of chloride. In chloride-containing electrolytes, the deposits were found to be sharper and denser compared to chloride-free ones.^[19,37,39,46] From the SEM images in Figure 6, it becomes clear that, as expected, the Mg morphology strongly depends on the Mg salt combination. A relatively close packing of Mg deposits is observed for the Mg(HMDS)₂/MgCl₂ electrolyte. In contrast to that, larger spherical crystallites are observed for the deposits from the Mg[B(hfip)₄]₂ electrolyte. For the Mg(TFSI)₂/MgCl₂, X-like structures are observed and the packing is less dense than for the deposits from the Mg(HMDS)₂/MgCl₂ electrolyte. As expected, Mg(HMDS)₂/MgCl₂ electrolyte with the highest Coulombic efficiency in the electrochemical experiments shows the smoothest and most compact plating and the least efficient Mg(TFSI)₂-based electrolyte the lowest. The XPS analyses in Figure 6 and Figure S14, Supporting Information, show that, besides the electrolyte residues, MgF₂ was present on the surface. After 15 min of sputtering, the signals in the F 1s spectrum related to the electrolyte salt (CF₃) vanished but the signals of MgF₂ were still present. This means that the reaction between deposited Mg and the Mg salts could have occurred, which lowered the Coulombic efficiency and had an influence on the morphology of the deposits. Compared to DME-based electrolytes from literature, similar species, such as fluorides, were found on the surface by XPS.^[19,39,48]

The fact that sharper deposits are observed in the chloride-containing DEGDEE electrolytes compared to the chloride-free electrolytes in Figure 6 is in agreement with the abovementioned observations in literature for other Mg electrolytes. Therefore, the addition of chloride to the Mg[B(hfip)₄]₂ electrolyte would have most probably also led to a smoother plating and more densely packed Mg deposits as it was observed in DME-based electrolytes.^[37] A close look with high magnification (Figure 6d–f) reveals that the crystallites consist of multiple layers in all three electrolytes.

3. Conclusion

To conclude, DEGDEE is broadly applicable as solvent for Mg electrolytes and is electrochemically as stable as DME. In combination with commonly used Mg salts, it enables Mg plating and stripping with a high Coulombic efficiency, comparable to the DME-based electrolytes. At the same time, the overpotentials are clearly higher due to a lower electrolyte conductivity. As for DME electrolytes, the morphology of electroplated Mg strongly depends on the Mg salt and the plated Mg is smoother and more compact when few side reactions between Mg and electrolyte occur. The application of DEGDEE in rechargeable Mg batteries would bring the benefit of an increase in battery safety due to the lower vapor pressure and higher flashpoint compared to DME and THF and being less harmful than DME, THF, and the higher glymes from today's perspective. However, challenges still need to be overcome, such as improving conductivity, so that the voltage hysteresis between charge and discharge voltages of the full RMB stays small. Further improvements could be tackled by the addition of inert conductive salts and the screening for

alternative Mg salts which are better soluble and show higher conductivity in combination with DEGDEE. Mg[B(hfip)₄]₂ appears to be a promising salt in combination with DEGDEE, which among further promising non-nucleophilic fluorinated Mg salts could be synthesized in DEGDEE to investigate the purely DEGDEE-based electrolytes. The combination of DEGDEE and DME in a mixed electrolyte would probably also be an option to combine the positive aspects of both solvents, especially the higher conductivity related to DME and the beneficial safety aspects of DEGDEE. With this work, we have expanded the range of available ether solvents for reversible electrochemical Mg deposition. Further, it also highlights the importance of the electrolyte solvent and motivates further research in this direction in order to achieve the ultimate goal of a practical and safe rechargeable Mg battery.

4. Experimental Section

Electrolyte Preparation

As solvents, DEGDEE (99%, Alfa Aesar) and DME (99.5%, Sigma-Aldrich) were used. Prior to use, both solvents were dried over molecular sieves (3 and 4 Å) for several days, which resulted in a water content below 10 ppm, tested by Karl–Fischer titration (KF-Coulometer 851 by Metrohm, with Hydranal Coulmat AG electrolyte by Honeywell). All chemicals were stored and the electrolytes were mixed under inert atmosphere (<0.5 ppm H₂O, <0.5 ppm O₂).

The electrolytes were prepared by mixing the respective Mg salts and TBABH₄ with DEGDEE and DME respectively. For the Mg(HMDS)₂-based DEGDEE electrolyte, 0.14 M Mg(HMDS)₂ (97%, Sigma-Aldrich), 0.14 M MgCl₂ (99.9%, Alfa Aesar), and 15 mM TBABH₄ (98%, Sigma-Aldrich) were mixed with dry DEGDEE and stirred at 40–60 °C for at least 24 h. For the Mg(HMDS)₂-based DME electrolyte, 0.1 M Mg(HMDS)₂ (97%, Sigma-Aldrich), 0.05 M MgCl₂ (99.9%, Alfa Aesar), and 15 mM TBABH₄ (98%, Sigma-Aldrich) were mixed with dry DME and stirred at 40–50 °C for at least 24 h.

For the Mg[B(hfip)₄]₂-based DEGDEE electrolyte, 0.14 M Mg[B(hfip)₄]₂·3DME^[44,64] and 20 mM TBABH₄ (98%, Sigma-Aldrich) were mixed with dry DEGDEE and stirred at 40–60 °C for at least 24 h. For the DME counterpart, the same molarity was dissolved in dry DME.

For the Mg(TFSI)₂-based DEGDEE electrolyte, 0.05 M Mg(TFSI)₂ (99.5%, Solvionic), 0.05 M MgCl₂ (99.9%, Alfa Aesar), and 15 mM TBABH₄ (98%, Sigma-Aldrich) were mixed with dry DEGDEE and stirred at 40–60 °C for at least 24 h. Mg(TFSI)₂ was dried under vacuum at 80 °C for 24 h prior to use.

Electrolyte conductivities were measured with the digital conductivity meter GMH 3410 (Greisinger electronic) at room temperature (21 °C). It has to be mentioned that the values were not completely stable, most probably due to the reaction of borohydride with contaminants, resulting in some gas formation. Therefore, we assumed an error of 10%.

Electrochemical Measurements

Cyclic voltammetry was performed in a three-electrode setup with a Swagelok-type Bola cell. A Pt foil (99.9%, MaTeCK Jülich, diameter 12 mm, 1.13 cm² geometrical electrode area) which was cleaned and annealed before use served as the working electrode. Mg wire with a diameter of 0.5 mm (99.9%, Goodfellow) was used as the reference electrode and Mg foil (99.9%, Goodfellow) as the counter

electrode. Both Mg electrodes were cleaned with a sand paper under inert atmosphere prior to use. Two glass fiber separators (Whatman, GF/B) with a diameter of 12 mm were used and the Mg reference electrode was placed between the two separators. Each separator was soaked with 60 μ L electrolyte, resulting in a total electrolyte volume of 120 μ L.

Galvanostatic measurements were performed in a two-electrode setup with a Swagelok-type Bola cell. A Pt foil (99.9%, MaTeck Jülich, diameter 12 mm, 1.13 cm² geometrical electrode area) which was cleaned and annealed before use served as the working electrode and a Mg foil which was cleaned with sand paper under inert atmosphere prior to use as the counter electrode. One glass fiber separator (Whatman, GF/B) with a diameter of 12 mm and soaked with an electrolyte volume of 60 mL was placed between the two electrodes.

All electrochemical measurements were performed with a BioLogic SP-300 potentiostat.

SEM/EDS/XPS

For the SEM measurements, the cell was disassembled in the glovebox after the electrochemical Mg deposition step. The Pt electrode was carefully immersed and rinsed in dry DEGDEE. Subsequently, the electrode was dried with a lint-free paper tissue and dried in the antechamber of the glovebox under vacuum. Afterward, the sample was transferred to the SEM and kept under vacuum overnight to eliminate any possible solvent residuals before the measurement. The images were recorded with the Quattro S (Thermo Fischer Scientific) using a secondary-electron mode and an acceleration voltage of 10 kV.

For the SEM/EDS measurements, the procedure was the same as for the SEM measurements. The SEM measurement was performed with the Scios 2 (Thermo Fisher Scientific) which was coupled with EDS (Ametek, USA).

For the X-ray Photoelectron spectroscopy (XPS) measurements, the Mg plating and cleaning of the samples was done with the same conditions as for the SEM images. The XPS spectra were recorded with a PHI 5800 Electron spectroscopy for chemical analysis (ESCA) system (Physical Electronics), using monochromatic Al K α radiation (1486 eV). The pass energy was 93.9 eV for the survey and 58.7 eV for the detailed spectra. The sputter gun worked with Ar ions and a voltage of 5 keV. In all spectra, the reference for the energies was the C1s peak which was set to 284.7 eV.

Acknowledgements

The authors thank Dr. Maximilian U. Cebelin, Dr. Attila Farkas, and Dr. Tanja Geng for fruitful and supportive discussions. The authors also thank Adam Reupert for experimental support. Further, support by the German Research Foundation (DFG) through the Cluster of Excellence POLiS (project ID 390874152) as well as the priority program SPP-2248 Polymer-based Batteries (Project ID 441209207) is gratefully acknowledged. We thank Core Facility EMMA at the University of Ulm for providing support and access to XPS instrumentation. The authors further thank Philipp Schuster for experimental support with the NMR measurements and the DFG with the project ID 445471845.

Conflict of Interest

The authors declare no conflict of interest.

Data Availability Statement

The data that support the findings of this study are available from the corresponding author upon reasonable request.

Keywords: battery safeties · diethylene glycol diethyl ethers · electrochemistries · electrolytes · rechargeable magnesium batteries

- [1] M. Armand, P. Axmann, D. Bresser, M. Copley, K. Edström, C. Ekberg, D. Guyomard, B. Lestriez, P. Novák, M. Petranikova, W. Porcher, S. Trabesinger, M. Wohlfahrt-Mehrens, H. Zhang, *J. Power Sources* **2020**, *479*, 228708.
- [2] M. Li, J. Lu, Z. Chen, K. Amine, *Adv. Mater.* **2018**, *30*, 1800561.
- [3] M. R. Palacin, *J. Phys. Energy* **2024**, *6*, 031501.
- [4] A. Ponrouch, J. Bitenc, R. Dominko, N. Lindahl, P. Johansson, M. R. Palacin, *Energy Storage Mater.* **2019**, *20*, 253.
- [5] Y. Tian, G. Zeng, A. Rutt, T. Shi, H. Kim, J. Wang, J. Koettgen, Y. Sun, B. Ouyang, T. Chen, Z. Lun, Z. Rong, K. Persson, G. Ceder, *Chem. Rev.* **2021**, *121*, 1623.
- [6] R. Deivanayagam, B. J. Ingram, R. Shahbazian-Yassar, *Energy Storage Mater.* **2019**, *21*, 136.
- [7] J. A. Blázquez, R. R. Maça, O. Leonet, E. Azaceta, A. Mukherjee, Z. Zhao-Karger, Z. Li, A. Kovalevsky, A. Fernández-Barquín, A. R. Mainar, P. Jankowski, L. Rademacher, S. Dey, S. E. Dutton, C. P. Grey, J. Drews, J. Häcker, T. Danner, A. Latz, D. Sotta, M. R. Palacin, J. F. Martin, J. M. G. Lastra, M. Fichtner, S. Kundu, A. Kraysberg, Y. Ein-Eli, M. Noked, D. Aurbach, *Energy Environ. Sci.* **2023**, *16*, 1964.
- [8] J. Muldoon, C. B. Bucur, T. Gregory, *Chem. Rev.* **2014**, *114*, 11683.
- [9] R. Attias, M. Salama, B. Hirsch, Y. Goffer, D. Aurbach, *Joule* **2019**, *3*, 27.
- [10] Z. Ma, D. R. MacFarlane, M. Kar, *Batter. Supercaps* **2019**, *2*, 115.
- [11] R. Mohtadi, F. Mizuno, *Beilstein J. Nanotechnol.* **2014**, *5*, 1291.
- [12] J. Song, E. Sahadeo, M. Noked, S. B. Lee, *J. Phys. Chem. Lett.* **2016**, *7*, 1736.
- [13] S. Y. Ha, Y. W. Lee, S. W. Woo, B. Koo, J. S. Kim, J. Cho, K. T. Lee, N. S. Choi, *ACS Appl. Mater. Interfaces* **2014**, *6*, 4063.
- [14] L. Wang, S. Riedel, Z. Zhao-Karger, *Adv. Energy Mater.* **2024**, *14*, 2402157.
- [15] H. Zhang, L. Qiao, M. Armand, *Angew. Chemie - Int. Ed.* **2022**, *61*, e202214054.
- [16] Z. Zhao-Karger, M. E. Gil Bardaji, O. Fuhr, M. Fichtner, *J. Mater. Chem. A* **2017**, *5*, 10815.
- [17] O. Mizrahi, N. Amir, E. Pollak, O. Chusid, V. Marks, H. Gottlieb, L. Larush, E. Zinigrad, D. Aurbach, *J. Electrochem. Soc.* **2008**, *155*, A103.
- [18] C. Liao, N. Sa, B. Key, A. K. Burrell, L. Cheng, L. A. Curtiss, J. T. Vaughey, J. J. Woo, L. Hu, B. Pan, Z. Zhang, *J. Mater. Chem. A* **2015**, *3*, 6082.
- [19] I. Shterenberg, M. Salama, H. D. Yoo, Y. Gofer, J.-B. Park, Y.-K. Sun, D. Aurbach, *J. Electrochem. Soc.* **2015**, *162*, A7118.
- [20] N. L. Grotkopp, M. Horst, G. Garnweitner, *Batter. Energy* **2024**, *3*, 20240002.
- [21] Y. Sun, F. Ai, Y. C. Lu, *Small* **2022**, *18*, 2200009.
- [22] S. Tan, J. Xu, R. Deng, Q. Zhao, C. Xu, G. Huang, J. Wang, F. Pan, *J. Energy Chem.* **2024**, *94*, 656.
- [23] Y. Man, P. Jaumaux, Y. Xu, Y. Fei, X. Mo, G. Wang, X. Zhou, *Sci. Bull.* **2023**, *68*, 1819.
- [24] Entry on 1,2-Dimethoxyethane in the GESTIS Substance Database of the IFA, <https://gestis-database.dguv.de/data?name=030730>, (accessed: March, 2025).
- [25] R. Dominko, J. Bitenc, R. Berthelot, M. Gauthier, G. Pagot, V. Di Noto, *J. Power Sources* **2020**, *478*, 229027.
- [26] K.-C. Lau, T. J. Seguin, E. V. Carino, N. T. Hahn, J. G. Connell, B. J. Ingram, K. A. Persson, K. R. Zavadil, C. Liao, *J. Electrochem. Soc.* **2019**, *166*, A1510.
- [27] T. Mandai, Y. Youn, Y. Tateyama, *Mater. Adv.* **2021**, *2*, 6283.
- [28] R. Jay, A. W. Tomich, J. Zhang, Y. Zhao, A. De Gorostiza, V. Lavallo, J. Guo, *ACS Appl. Mater. Interfaces* **2019**, *11*, 11414.
- [29] Z. Ma, M. Kar, C. Xiao, M. Forsyth, D. R. MacFarlane, *Electrochem. Commun.* **2017**, *78*, 29.
- [30] Entry on Diethylene glycol dimethyl ether in the GESTIS Substance Database of the IFA, <https://gestis-database.dguv.de/data?name=037380>, (accessed: March 2025).
- [31] S. Su, Y. NuLi, N. Wang, D. Yusipu, J. Yang, J. Wang, *J. Electrochem. Soc.* **2016**, *163*, D682.

- [32] T. Mandai, K. Tatesaka, K. Soh, H. Masu, A. Choudhary, Y. Tateyama, R. Ise, H. Imai, T. Takeguchi, K. Kanamura, *Phys. Chem. Chem. Phys.* **2019**, *21*, 12100.
- [33] G. A. Giffin, *J. Mater. Chem. A* **2016**, *4*, 13378.
- [34] S. Fang, G. Wang, L. Qu, D. Luo, L. Yang, S. I. Hirano, *J. Mater. Chem. A* **2015**, *3*, 21159.
- [35] Entry on Diethylene glycol diethyl ether in the GESTIS Substance Database of the IFA, <https://gestis-database.dguv.de/data?name=012750>, (accessed: March 2025).
- [36] S.-M. Han, J.-H. Kim, D.-W. Kim, *J. Electrochem. Soc.* **2014**, *161*, A856.
- [37] B. Dlugatch, J. Drews, R. Attias, B. Gavriel, A. Ambar, T. Danner, A. Latz, D. Aurbach, *J. Electrochem. Soc.* **2023**, *170*, 090542.
- [38] R. Horia, D. T. Nguyen, A. Y. S. Eng, Z. W. Seh, *Nano Lett.* **2021**, *21*, 8220.
- [39] L. Leuppert, A. Reupert, T. Diemant, T. Philipp, C. Kranz, Z. Li, M. Fichtner, *RSC Appl. Interfaces* **2024**, *1*, 1142.
- [40] R. Horia, D. T. Nguyen, A. Y. S. Eng, Z. W. Seh, *Batter. Supercaps* **2022**, *5*, e202200011.
- [41] D. Chinnadurai, W. Y. Lieu, S. Kumar, G. Yang, Y. Li, Z. W. Seh, *Nano Lett.* **2023**, *23*, 1564.
- [42] Z. Liang, C. Ban, *Angew. Chemie Int. Ed.* **2021**, *133*, 11136.
- [43] H. D. Yoo, S. D. Han, I. L. Bolotin, G. M. Nolis, R. D. Bayliss, A. K. Burrell, J. T. Vaughey, J. Cabana, *Langmuir* **2017**, *33*, 9398.
- [44] Z. Zhao-Karger, R. Liu, W. Dai, Z. Li, T. Diemant, B. P. Vinayan, C. Bonatto Minella, X. Yu, A. Manthiram, R. J. Behm, M. Ruben, M. Fichtner, *ACS Energy Lett.* **2018**, *3*, 2005.
- [45] Z. Yang, L. Gao, N. J. Leon, C. Liao, B. J. Ingram, L. Trahey, *ACS Appl. Energy Mater.* **2024**, *7*, 1666.
- [46] B. W. Schick, V. Vanoppen, M. Uhl, M. Kruck, S. Riedel, Z. Zhao-Karger, E. J. Berg, X. Hou, T. Jacob, *Angew. Chem. Int. Ed.* **2024**, *63*, e202413058.
- [47] F. Tuerxun, Y. Abulizi, Y. NuLi, S. Su, J. Yang, J. Wang, *J. Power Sources* **2015**, *276*, 255.
- [48] Z. Li, T. Diemant, Z. Meng, Y. Xiu, A. Reupert, L. Wang, M. Fichtner, Z. Zhao-Karger, *ACS Appl. Mater. Interfaces* **2021**, *13*, 33123.
- [49] R. Attias, B. Dlugatch, O. Blumen, K. Shwartsman, M. Salama, N. Shpigel, D. Sharon, *ACS Appl. Mater. Interfaces* **2022**, *14*, 30952.
- [50] B. D. Adams, J. Zheng, X. Ren, W. Xu, J. G. Zhang, *Adv. Energy Mater.* **2018**, *8*, 1702097.
- [51] T. J. Seguin, N. T. Hahn, K. R. Zavadil, K. A. Persson, *Front. Chem.* **2019**, *7*, 175.
- [52] A. Kopač Lautar, J. Bitenc, T. Rejec, R. Dominko, J. S. Filhol, M. L. Doublet, *J. Am. Chem. Soc.* **2020**, *142*, 5146.
- [53] J. S. Lowe, D. J. Siegel, *J. Phys. Chem. C* **2018**, *122*, 10714.
- [54] T. Pavčnik, M. Lozinšek, K. Pirnat, A. Vizintin, T. Mandai, D. Aurbach, R. Dominko, J. Bitenc, *ACS Appl. Mater. Interfaces* **2022**, *14*, 26766.
- [55] N. Sa, N. N. Rajput, H. Wang, B. Key, M. Ferrandon, V. Srinivasan, K. A. Persson, A. K. Burrell, J. T. Vaughey, *RSC Adv.* **2016**, *6*, 113663.
- [56] O. Tutusaus, R. Mohtadi, T. S. Arthur, F. Mizuno, E. G. Nelson, Y. V. Sevryugina, *Angew. Chemie* **2015**, *127*, 8011.
- [57] C. Holc, K. Dimogiannis, E. Hopkinson, L. R. Johnson, *ACS Appl. Mater. Interfaces* **2021**, *13*, 29708.
- [58] J. Muldoon, C. B. Bucur, A. G. Oliver, J. Zajicek, G. D. Allred, W. C. Boggess, *Energy Environ. Sci.* **2013**, *6*, 482.
- [59] J. Drews, P. Jankowski, J. Häcker, Z. Li, T. Danner, J. M. García Lastra, T. Vegge, N. Wagner, K. A. Friedrich, Z. Zhao-Karger, M. Fichtner, A. Latz, *ChemSusChem* **2021**, *14*, 4820.
- [60] A. Baskin, D. Prendergast, *J. Phys. Chem. C* **2016**, *120*, 3583.
- [61] V. Prabhakaran, G. Agarwal, J. D. Howard, S. Wi, V. Shutthanandan, D. T. Nguyen, L. Soule, G. E. Johnson, Y. S. Liu, F. Yang, X. Feng, J. Guo, K. Hankins, L. A. Curtiss, K. T. Mueller, R. S. Assary, V. Murugesan, *ACS Appl. Mater. Interfaces* **2023**, *15*, 7518.
- [62] T. Fukutsuka, K. Asaka, A. Inoo, R. Yasui, K. Miyazaki, T. Abe, K. Nishio, Y. Uchimoto, *Chem. Lett.* **2014**, *43*, 1788.
- [63] S. Yagi, A. Tanaka, Y. Ichikawa, T. Ichitsubo, E. Matsubara, *Res. Chem. Intermed.* **2014**, *40*, 3.
- [64] W. Ren, D. Wu, Y. Nuli, D. Zhang, Y. Yang, Y. Wang, J. Yang, J. Wang, *ACS Energy Lett.* **2021**, *6*, 3212.

Manuscript received: February 2, 2025

Revised manuscript received: March 11, 2025

Version of record online: